

## Cleavage-Ductile Fracture Transition Study by Competition Between Two Fracture Criteria

D. Bouche

*E.N.S.M.P., 60 Bd. Saint Michel, F-75272 Paris Cedex 06, France*

D. Dubois

*Framatome, Division des Fabrications, B.P. No. 13, F-71380 Saint Marcel, France*

M. Bretin

*Creusot-Loire, Laboratoire du Creusot, F-71200 Le Creusot, France*

### Abstract

The susceptibility to fracture of engineering materials is generally tested by creating temperature conditions for which the expected fracture mode is definitely brittle or ductile.

At an intermediate range of temperature where the processes of crack production and accommodation by local slip compete, a transition from brittle to ductile will occur.

The goal of this paper is to present the results of a comprehensive programme in which experiments and numerical simulations have been jointly conducted :

A508 steel axi-symmetrical test specimens have been fractured at -90 degrees C and macrofractographic examinations have been performed ; the numerical simulation has been carried out by running a finite element programme (TITUS) using an updated Lagrangian formulation and fracture modes have been estimated from brittle and ductile fracture local criteria, respectively based on Weibull statistics and the Rice and Tracey approach.

The results predict the ductile initiation and propagation of cracks at the center of the specimens prior to final cleavage ; in addition the final rupture by brittle propagation is all the more retarded as the test specimen is smaller.

These results are fully confirmed by the experimental programme ; the ambiguity observed for AE2 notched specimens for which both criteria attain critical values is even cleared up by triaxiality considerations.

## 1. Introduction

The conception of pressure vessels is currently based on global criteria allowing the assertion of their integrity ; for temperatures within the transition range, the failure of these criteria can be compensated for by using local fracture criteria which have already been qualified for both ductile and brittle behaviors.

In this report, we present the results of the numerical simulation of rupture experiments conducted at -90 degrees C on A508 axisymmetrical test-specimens ; the calculations have been performed with a finite element programme (TITUS) with an updated lagrangian formulation ; moreover, the post-processing procedures of this programme can evaluate local fracture criteria.

We are indebted to F. Mudry for his most helpful contribution [1].

## 2. Description of Criteria

### 2.1 Brittle fracture criterion

The criterion is based on Weibull statistics [2] and has recently been extended [1] ; it is mathematically expressed as a rupture probability  $P(R)$  defined by:

$$P(R) = 1 - \exp(-(\sigma_w/\sigma_u)^m) \quad (1)$$

where  $\sigma_w$  (the Weibull stress) is defined by:

$$\sigma_w = \sqrt[m]{\int_{P.A} \sigma_I^m \cdot \exp(-m \cdot \epsilon_{eq}/2) dv/V0} \quad (2)$$

$\sigma_I$  is the maximum principal stress and  $\epsilon_{eq}$  the total strain ;  $m$ ,  $\sigma_u$  and  $V0$  are Weibull model parameters, and the integral is evaluated on the Plastic Area (P.A)

The previously observed effect of plastic deformation [1] has been introduced in the calculation of the Weibull stress ; in addition, the model contains only 2 independent parameters ( $m$  and  $V0^{1/m} \cdot \sigma_u$ ) indicating that the probability of rupture is zero only if the stress is zero.

The determination of  $m$ ,  $V0$  and  $\sigma_u$  has already been attempted and the values selected in this paper are similar to those previously obtained [1-3] :

$$V0 = 1.25 \cdot 10^{-4} \text{ mm}^3 \quad (\text{volume of cube with edge 50 microns})$$

$$m = 22$$

$$\sigma_u = 2630 \text{ MPa}$$

## 2.2 Ductile fracture criterion

The criterion of ductile fracture is based on the concept of a critical growth rate of holes ;the mechanism leading to rupture consists of 3 phases :

- decoherence by disbonding of inclusions based on Eshelby' theory [4] extended to the case of plastic deformation [5].
- growth of holes based on Rice and Tracey model [6], modified [7] to take into account the hardening properties of materials.
- initiation by coalescence of holes when the growth rate reaches a critical value.

The corresponding phases are computed with the following formulae :

- decoherence criterion :  $\sigma_I + 1.6(\sigma_{eq} - \sigma_0) = \sigma_c$  (3)

$\sigma_{eq}$  is the equivalent Von Mises stress,  $\sigma_0$  is the yield strength and  $\sigma_c$  is a critical stress ( $\sigma_c = 1120$  MPa [1])

- hole growth criterion :  $\text{Log}(R/R0) = \int_{\epsilon_{\text{decoherence}}}^{\epsilon_{\text{max}}} .28 \exp(1.5 \sigma_m / \sigma_{eq}) d\epsilon_{eq}$  (4)

$\sigma_m$  is the hydrostatic stress  $\sigma_m = \sigma_{ii} / 3$

- coalescence criterion :  $R/R0 = (R/R0)_c = 1.8$  [1]

## 3. Experimental Programme

Tensile test-specimens, homothetic notched specimens ( $\phi = 3.33, 6.66, 10, 13.33$  mm) and AE2 notched specimens have been fractured at -90 degrees C.

During the experiments, the temperature steadiness has been controlled and the variation of both minimum diameter and total length has been measured and the resulting load-displacement curves have been plotted.

All specimens have undergone very large plastic deformations :

- 70 % for homothetic specimens
- 25 and 40 % for AE2 specimens

(the same experiments were previously conducted at -196 degrees C :

- AE2, AE10 and AE13.33 specimens were fractured with a deformation less than 3%

- AE3.33 and AE6.66 specimens were fractured with higher strains (13% - 25% range) ; the examination of the surface revealed a cleavage facies despite the elevated plastic deformation).

#### 4. Finite Element Simulation

The finite element calculations are mainly concentrated on the simulation in the transition range (-90 degrees C) ; however we will give additional information at -196 degrees C on Weibull criterion results.

The homothetic feature of most specimen geometries can be rendered by a single numerical simulation and experimental results can further be compared to the finite element ones by an appropriate transformation. Results of homothetic specimen ( $\lambda$  ratio) will be compared to AE10 specimen after transformation of P-DL and P-DPHI curves into  $P/\lambda^2 - DL/\lambda$  and  $P/\lambda^2 - DPHI/\lambda$  curves ( $DPHI = \phi_0 - \phi$ ).

The calculations are carried out for an AE10 specimen and for an AE2 specimen whose geometries and meshes are plotted in figures 1 and 2 respectively.

The scatter in the constitutive relations determined from diameter and length variations drives us to perform most calculations with 2 laws (called hard law and soft law).

The resulting curves are plotted on fig.3 on which the evolution of the mean stress (P/S) estimated from homothetic specimen experiments as a function of the total strain ( $\epsilon = 2 \text{ LOG } \phi_0 / \phi$ ) is also represented : the discrepancy appearing with larger specimens (AE10 and AE13.33) is attributed to the lack of ability for gauges to locate and measure the minimum diameter.

Nevertheless the precision of the numerical results is clearly expressed on figures 4 and 5 for P-DL and P-DPHI curves.

P-DL curves indicate that the soft law calculations are better suited to AE10 and AE13.33 specimens and that the hard law is more relevant to smaller specimens.

The comparison with the maximum forces and associated displacements is fairly good:

	Pmax N	DL microns
law 1	70820	960
law 2	67590	910
AE10 exp 1	67400	960
AE10 exp 2	66800	960
AE6.66	70700	(9/4*31360 by homothetic comparison)

P-DPHI curves yield identical results; the estimated diameter variations were respectively 780 (law 1) and 705 microns (law 2) for 700 microns actually measured.

These same experiments were simulated with mechanical properties at -196 degrees C in order to validate the Weibull criterion ; the numerical simulation of the AE2 specimen yielded very satisfactory results : a probability of failure of 91% for a total strain less than 2%.

### 5. Results and Discussion

The distribution of the damage function  $R/R_0$  in the minimum section is plotted on fig. 6 for AE10 and AE2 specimens, for both laws, and at the estimated maximum strain before rupture.

- For the AE10 specimen, the maximum strain reaches 67 % and the maximum value of  $R/R_0$  is situated on the axis and exceeds the threshold of coalescence ; in addition, the computed Weibull stress ( $\sigma_w = 2000$  MPa) indicates a brittle fracture probability of less than 0.2 %.

The history predicted by the numerical simulation is then : the ductile initiation occurs on the axis of the specimen in the minimum section ; the ductile propagation of the crack reduces the remaining ligament thus increasing the average stress level and consequently the Weibull stress (the propagation could be simulated by using a node release technique).

The estimation of the Weibull stress during the propagation can be easily made since the load does not vary very much before failure ; the stress is then inversely proportional to the remaining ligament surface:

$$\sigma_w = \sigma_{w0} \cdot R^2/(R^2-r^2) \quad \text{with } \sigma_{w0} = 2000 \text{ MPa}$$

when  $\sigma_w = \sigma_u$ , the brittle fracture probability reaches 55% and the corresponding value of  $r$  is :  $r = 0.48 R$

This same probability extended to homothetic specimens is expressed by :

$$\sigma_{w(\lambda)} = \lambda^{3/m} \sigma_{w(1)}$$

the same rupture probability is obtained for :

$$1.3/\lambda^{3/m} = 1 - (r/R)^2$$

in the case of the AE3.33 specimen this condition yields  $r = 0.6 R$

The ductile zone is then predicted proportionally greater on the smaller specimens ; however the steep increase of the brittle fracture probability with  $\sigma_w$  when  $\sigma_w$  exceeds  $\sigma_u$  indicates that the final rupture of all specimens will be brittle.

The experiments confirm these predictions:

the macrofractographic examinations display a ductile cup facies at the center of most specimens ; some off-centre positions can be observed and are related to the presence of oxides (figures 7 to 12). The ductile initiation is all the more important as the specimen is smaller and in the case of the AE3.33 the ductile zone stretches over almost all the fractured area.

- In the case of the AE2 specimen for which the hard law is best suited the maximum value of R/RO (1.73) is also situated on the axis ; for the same load, the brittle fracture probability reaches 77 % ; the ductile decoherence has occurred but one may have a hard time sorting out the winner of the competition on these crude results.

However, an increasing triaxiality has been proved to entail a loss of ductility in materials by reducing the critical growth of cavities : the computed triaxiality of AE2 specimens has been calculated to be twice that obtained on AE10 specimens [8] and results of reference [1] indicate that for these former specimens the critical value of R/RO is 1.69. With this new value, the coalescence criterion is met while the brittle fracture probability is lower : the numerical simulation predicts again the ductile initiation and is consistent with the experimental results.

#### References

- [1] MUDRY, F., Ductile and Brittle fracture of low alloy steels  
Ph D thesis on Physical Sciences, Ecole des Mines de Paris
- [2] WEIBULL, W., Journal of applied mechanics (1951)
- [3] WESTINGHOUSE, Report WA NL-TME-2688
- [4] ESHELBY J., Proceedings of the Royal Society (1957), a 241, p 376
- [5] BERVEILLER M., ZAOUÏ A., Journal of the Mechanics and Physics of solids (1979), vol 26, page 325
- [6] RICE J. R., TRACEY D. M., Journal of the Mechanics and Physics of solids (1969), vol. 17 page 201
- [7] HILL R., The mathematical theory of plasticity, Clarendon Press Oxford 1950
- [8] MOTTET G., Numerical simulation of AE2 AE4 AE10 test-specimens  
Framatome Internal Publication TM/C DC/80.095

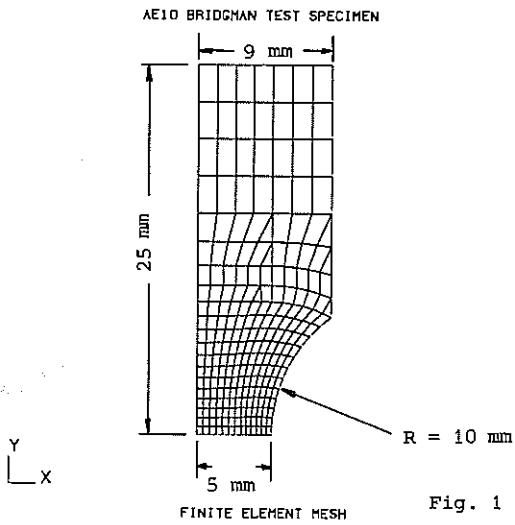


Fig. 1

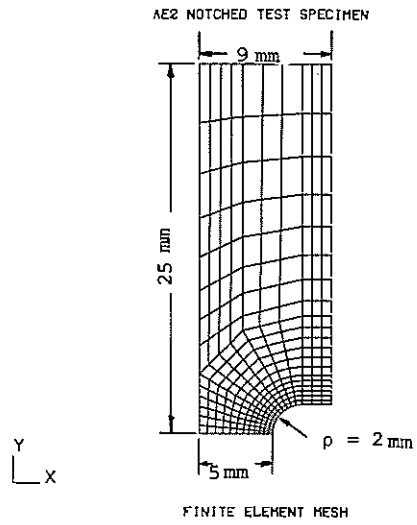


Fig. 2

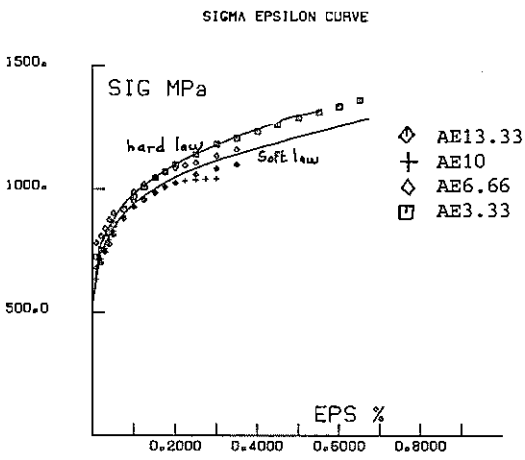


Fig. 3

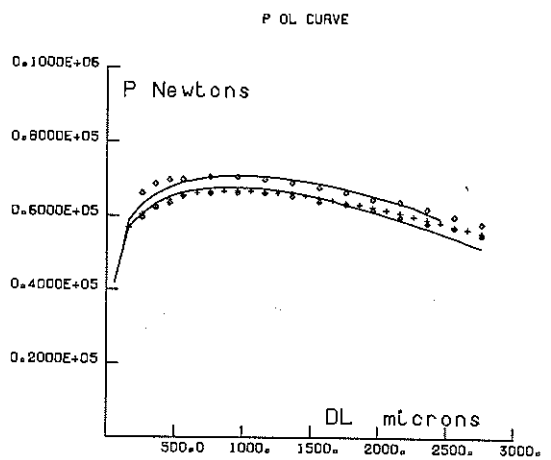
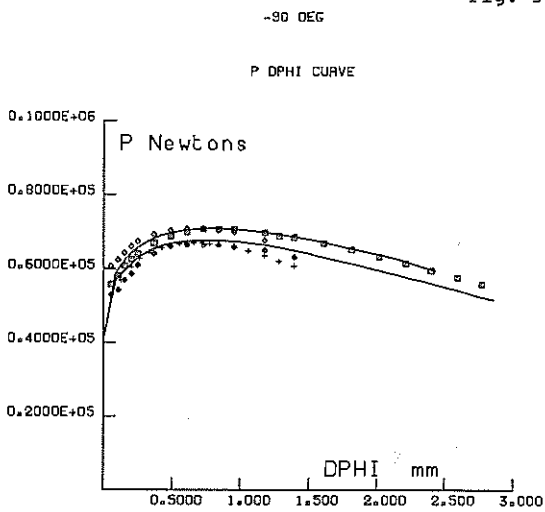
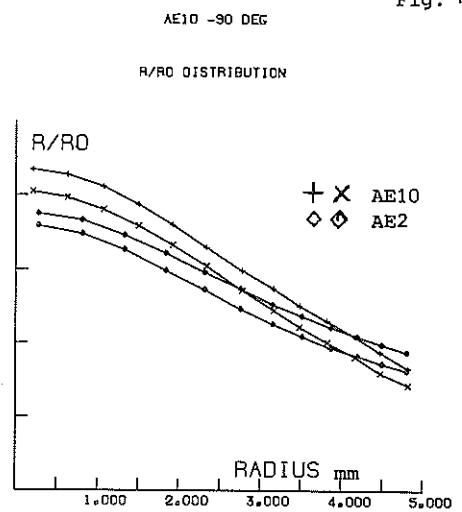


Fig. 4



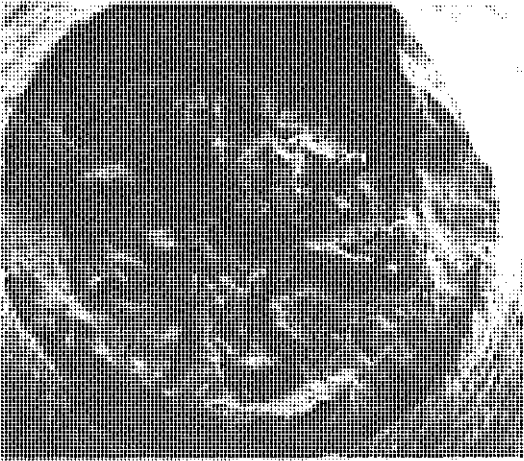
AE10 -90 DEG

Fig. 5



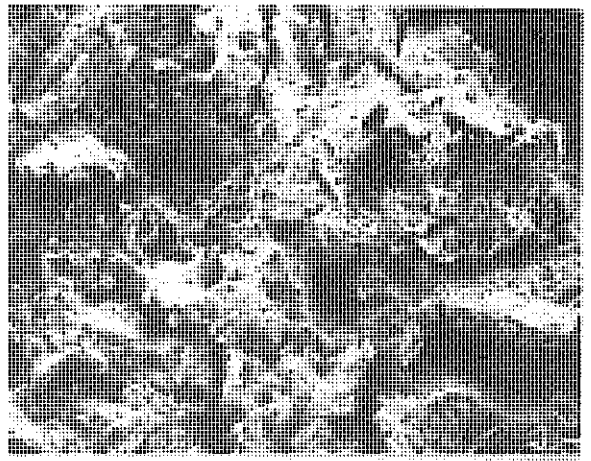
AE2 AND AE10 TEST-SPECIMENS T=-90 DEG

Fig. 6



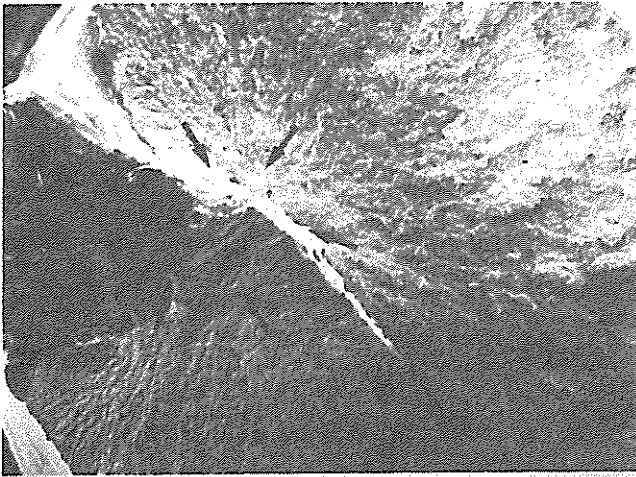
AE 3.33 (X 50)

Fig. 7



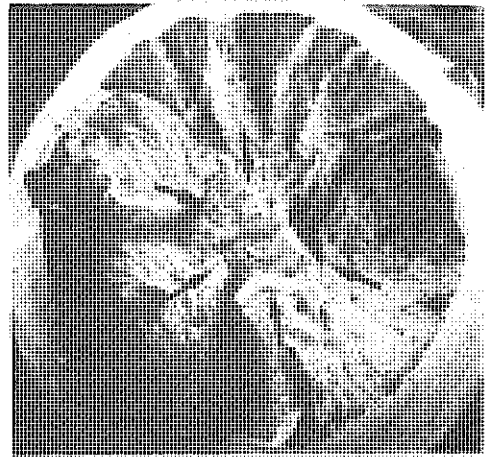
AE 3.33 (X 100)

Fig. 8



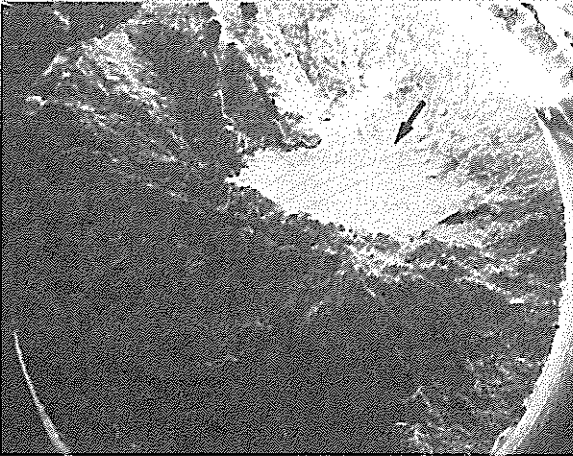
AE 13.33 (X 15)

Fig. 9



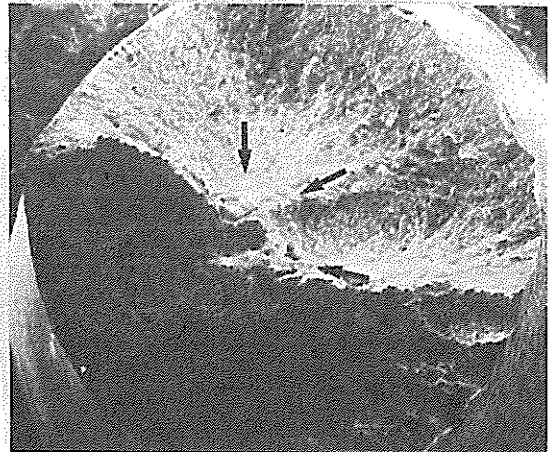
AE 6.66 (X 20)

Fig. 10



AE 2 (X 15)

Fig. 11



AE 10 (X 15)

Fig. 12